P8.7 – POLARIMETRIC RADAR CHARACTERISTICS OF A SUPERCELL HAILSTORM ON 10 MAY 2010 IN CENTRAL OKLAHOMA

CLARK D. PAYNE[1,2] * , C.A. VAN DEN BROEKE[1,2], L.R. LEMON[1,2], P.T. SCHLATTER[2]

[1] *Cooperative Institute for Mesoscale Meteorological Studies (CIMMS), Norman, OK*

[2] *NOAA/NWS/Warning Decision Training Branch, Norman, OK*

1. Introduction

The dual-polarization signatures of hail have been well-studied since the 1970s (Bringi and Chandrasekar (2001)). In particular, this study will focus on the dual-polarization signatures in giant hail (defined here as hail with equivolume diameter > 4 cm). Before diving into the observations, we'll present a short review on the polarimetric variables and the physical and polarimetric characteristics of hail.

a. *Polarimetric Variables*

Currently, the Weather Surveillance Radar - 1988 Doppler (WSR-88D) network provides the following base moments: reflectivity (Z), radial velocity (V) and spectrum width (σ_v). With a dual-polarization Doppler radar, these base moments will also be produced along with the following variables: differential reflectivity (Z_{DR}), differential phase shift (Φ_{DP}), and cross-correlation coefficient (ρ_{HV}). One thing to note with ρ_{HV} is that in the operational community it will be known as CC. Since this paper is geared more for operational meteorologists, we will use CC. Differential reflectivity is a good indicator of the reflectivity-weighted median drop-size diameter (Herzegh and Jameson (1992)). The Φ_{DP} is defined as the difference in the attenuation rates of the horizontal and vertical pulses. However, a more meteorologically useful quantity is the range derivative of the Φ_{DP} which is called the specific differential phase (K_{DP}). The K_{DP} is a good indicator of the liquid water content and rain rate (Sachidananda and Zrnic (1986)). Another note, operational meteorologists will not be able to view Φ_{DP} in their display software called the Advanced Weather Interactive Processing System (AWIPS). Finally, the CC is a measure of how similarly the horizontal and vertical pulses behave from pulse-to-pulse within a resolution volume. It is best at discriminating between meteorological (CC > 0.9) and non-meteorological echoes (CC < 0.85). For more information on the polarimetric variables, refer to Doviak and Zrnic (1993) and Straka et al. (2000).

b. *Physical Characteristics of Giant Hail*

The physical characteristics which are important in dual-polarization signatures are shape, particle density and fall orientation.

The shape of giant hail can be quite complex. Bringi and Chandrasekar (2001) noted that the most common shape of large hail is an oblate spheroid. List (1986) also supported this idea of giant hail being an oblate spheroid, but also mentioned that giant hail can be irregularly shaped with small or large protuberances. An extensive study by Knight (1986) showed that the most common axis ratio for giant hail that can be modeled as oblate was approximately 0.6 to 0.8. The axis ratio is defined as the ratio between the minor axis and the major axis.

Lesins and List (1986) reported in their observations that giant hail tends to be dry. However, as the hail fell below the melting level, the hail began to melt and that melt water either remained on, or shed off the hailstone. Modeling results by Rasmussen et al. (1984) showed that hail larger than 9 mm in diameter shed the water that develops on the melting hail, while hail smaller than 9 mm will retain the meltwater and develop a water torus.

The last characteristic, fall orientation, is the least well-understood of all the physical characteristics. Knight and Knight (1970) and Steinhorn and Zrnic (1988) suspected that giant hail, on occasion, falls with its major axis in the vertical. However, modeling results by Zrnic et al. (1993) showed that hail with D > 4 cm falls with its major axis in the horizontal. Finally, other studies showed that giant hail tends to tumble (i.e. Knight and Knight (1970) and Lesins and List (1986))

c. *Polarimetric Characteristics of Giant Hail*

Beginning with reflectivity (Z), Mason (1971) noted that a lower threshold for hail is typically 55 dBZ. Since Z is dependent upon the sixth power of the diameter of the target,

**Corresponding author address:* Clark Payne
120 David L. Boren Blvd Suite 2640
Norman, OK 73072
Email: clark.payne@noaa.gov

it follows that giant hail should have Z > 55 dBZ. And, according to Straka et al. (2000), giant hail should have reflectivity between 60 and 80 dBZ unless it is dry in which case reflectivity could be as low as 45 dBZ.

Differential reflectivity in giant hail is not as simple to understand as reflectivity. Knight and Knight (1970) and Steinhorn and Zrnic (1988) both suspected that giant hail fell with its major axis in the vertical which helped them explain the resulting negative Z_{DR}values. However, a modeling study by Zrnic et al. (1993) showed that giant hail tends to fall horizontally-oriented yet still have negative Z_{DR}. This apparent discrepancy of Z_{DR} in giant hail is caused by Mie scattering effects (Aydin and Zhao (1990); Longtin et al. (1987); Melnikov et al. (2010)). A more recent study by Kumjian et al. (2010) has further complemented these this apparent discrepancy in Z_{DR} by looking at the effects on Z_{DR} due to melting. Their results showed that dry hailstones have a peak in positive Z_{DR} followed by a switch in sign of Z_{DR} near an equivolume diameter of 4.5 to 5.5 cm. If the hailstone has begun to melt, these effects are amplified due to its increased dielectric constant and occurs at diameters near 3 to 4 cm.

While most studies have focused on the Z_{DR} values of hail, a paper by Balakrishnan and Zrnic (1990) described the effects of hail size, distribution, canting angle, etc. on the correlation coefficient. Their results showed that CC tends to decrease as the hail size increases, protuberances-to-diameter ratio increases, hail size distribution increases, hail becomes wet/spongy, and hail mixes with other hydrometeors. The primary effect to note here is wet versus dry hail. Balakrishnan and Zrnic (1990) showed that if hail is dry, there is little effect on CC as hail size increases. However, there is a substantial decrease in CC when the diameter of hail is around 5 cm for wet/spongy hail. An operational assessment of polarimetric data was conducted during JPOLE which showed that in a severe storm that produced greater than 13 cm hail, the CC in that storm dropped to as low as 0.7 (Scharfenberg et al. (2005))

2. Data & Analysis

The day of 10 May 2010 was ideal for hail-producing, tornadic supercell thunderstorms. The environment was characterized by high shear and high CAPE (Van Den Broeke et al. (2010)). The location of the Moore hailstorm was such that it passed within 25 km to the north of the KOUN polarimetric radar located in Norman, OK. The close proximity of the storm to KOUN and the storm reports received on this day form the basis for this paper. The KOUN radar and the source for storm reports will be described below.

a. *KOUN*

The KOUN radar on 10 May 2010 was a test WSR-88D radar that had been upgraded to dual-polarization capabilities. However, since it was in a testing mode on this day, the data quality was not guaranteed to be of the same caliber as an operational WSR-88D. In fact, the radar was turned on just minutes before the event began and Z_{DR} was not calibrated. The result of this calibration yielded a Z_{DR} product that appeared to be too low. One of the authors visually inspected the data in areas of suspected dry snow which should have a Z_{DR} near 0.2 dB (Doviak and Zrnic (1993); Bringi and Chandrasekar (2001)), and noted that the Z_{DR} was indeed too low. Therefore, the data were corrected for this miscalibration by adding a 0.35 dB correction to all bins. The other dual-polarization variables (CC and K_{DP}) appeared to be well calibrated.

In addition to the miscalibration adjustment, the data in this study were Level 2 data sent from the radar data acquisition (RDA) unit to the radar product generator (RPG) where it was processed for viewing in AWIPS. Z_{DR} was first reduced from super-resolution down to a resolution of 0.25km x 1 deg. It was then smoothed using a five-gate spatial average filter and then was also corrected for attenuation and system calibration to create the processed Z_{DR} seen in AWIPS. CC was also reduced in resolution from super-resolution down to 0.25km x 1 deg. Lastly, reflectivity was unaltered from the RDA as it is seen in AWIPS. Since K_{DP} is not computed for CC below 0.9 and the majority of this analysis will be looking at regions of CC < 0.9, K_{DP} will not be discussed even though it will be shown in the figures.

b. *Storm Reports*

The storm reports were taken directly from the National Weather Service's (NWS) verification website (https://verification.nws.noaa.gov/). Despite the storm passing over a populated metropolitan area, there were a lack of hail reports. Some reasons for this might be because these storms were tornadic and people were taking shelter, and because the hail was so large that people were not willing to risk getting hurt in order to make measurements and send in reports. Also, some of the reports appear to have an error in the reported time. Therefore, the authors have adjusted some reports for this error in time based on subjective radar analysis.

3. Observations

The Moore, OK storm developed in far SW Caddo County in Oklahoma around 2100 UTC. It began as the far southern storm of a small, multicell cluster. At 2135 UTC, the far southern storm appeared to merge with the storm to its north and become the dominant storm. Approximately 10 minutes later, new development on the southern side of this merger appeared. This new development rapidly merged with the dominant storm around 2150 UTC and entered into the Oklahoma City metro area. The storms prior to 2150 UTC had a history of producing severe-sized hail, and had well-pronounced mesocyclones. The storm that progressed across the Oklahoma City metro area produced up to softball-sized hail and an EF-4 tornado.

This study will take a look at the time period between 2151 UTC and 2245 UTC noting the dual-polarization variable fields as the storm evolved and produced softball-sized hail that was reported. Discussion of the dual-polarization variables will be limited only to the 0.5 degree elevation angle. Future work will focus on a more volumetric analysis. As Kumjian et al. (2010) noted, melting hail can have extreme effects on the polarimetric signatures. Therefore, it is important to know the melting level when analyzing dual-polarization variables, thus the melting level on this day was 4.2 km. This was determined from a special sounding taken from Norman, OK at 2100 UTC. There will be no discussion on the EF-4 tornado in this paper. For more detail on the tornadoes of this day, refer to Lemon et al. (2010).

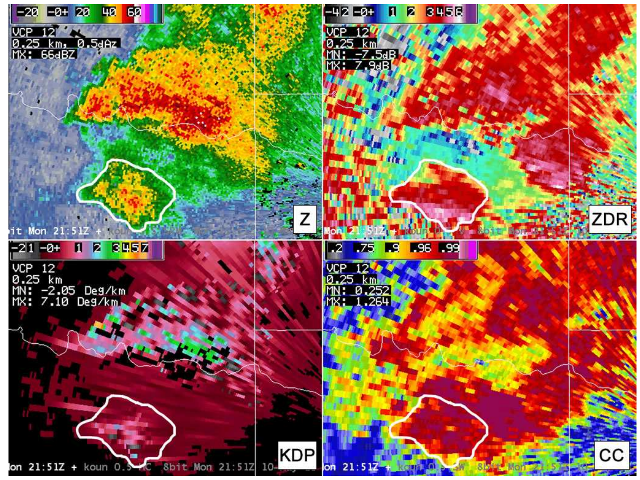

Figure 1: Reflectivity (Z; top left), Differential Reflectivity (Z_{DR}; top right), Cross-Correlation Coefficient (CC; bottom right), and Specific Differential Phase (K_{DP}; bottom left) for the time period 2151 UTC on 10 May 2010. The thick white bounded line represents the area of interest.

a. *2151 UTC*

At this time, the storm of interest is outlined by a white line in Figure 1. Reflectivity values are mostly near 40-50 dBZ, but a reflectivity gradient is developing on the southern flank. Z_{DR} values are all above 2 dB indicating large rain drops. However, one feature to note is the Z_{DR} arc (Kumjian and Ryzhkov (2008)). This signature indicates that the storm is encountering some enhanced low-level storm-relative helicity and might become supercellular soon. Lastly, CC are all above 0.97 for this storm.

No indication of giant hail in the low levels appears at this time in reflectivity. The dual-polarization variables also give us no indication of giant hail. The high Z associated with high Z_{DR} and high CC all indicate that in the low levels, only rain is reaching the surface at this time.

b. *2159 UTC*

The storm of interest has intensified from 2151 UTC. The reflectivity field has a larger area of greater than 50 dBZ. The main feature to note though is the change in the CC at the low levels. Whereas at 2151 UTC, the CC values were all greater than 0.97, at this time CC values at the low-levels have dropped significantly (near or below 0.9). This area of reduced CC is enclosed by a white line in Figure 2. This substantial reduction in CC is associated with a reduction in Z_{DR} and appears along the reflectivity gradient on the inflow side of the storm.

To avoid any possible reduction in CC due to low signal-to-noise ratio (SNR), only regions of $Z > 20$ dBZ were examined. In this region of good signal, there is no reason to suspect non-meteorological contamination which would lower the CC, so the low CC in good signal is assumed to be meteorological. The only meteorological situations in which CC drops this low is the melting of snow/graupel and giant, wet/spongy hail. Since we are examining the low-levels (< 0.5 km AGL) and the height of the melting layer is at approximately 4 km, we can safely assume melting snow is not causing this signature. Therefore, giant hail appears to be the culprit in this signature. Giant hail also makes sense because this signature is occurring along the reflectivity gradient near the inflow notch which is very near the updraft for the storm.

c. *2216 UTC*

The Moore, OK storm has now merged with the northern storm and has taken on classic supercellular characteristics noted in Lemon and Doswell (1979). Like the previous analysis time, we have marked two regions of reduced CC with white lines in Figure 3. The CC in these regions has dropped even lower than at 2159 UTC with values becoming as low as 0.7! Z_{DR} in these regions has also further decreased, becoming negative in some areas. Reflectivity has not increased much, with only a few pixels near or above 60 dBZ. Most of the area remains in the 45-55 dBZ range.

There were hail reports with this analysis time which was also the only time period where hail reports were received for this storm. All the hail reports resided along and within the eastern white bounded region noted in Figure 3. The decreased (and negative) Z_{DR} associated with the lowered CC are the main features to note with the observed giant hail. This is most likely caused by resonance effects noted

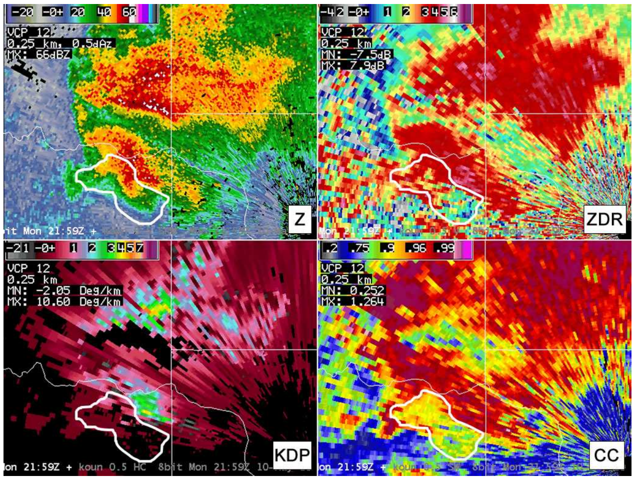

Figure 2: Same as Figure 1, but for 2159 UTC.

in past and recent modeling studies (Balakrishnan and Zrnic (1990); Kumjian et al. (2010); Melnikov et al. (2010)). Applying the signatures associated with the hail reports seen here, it can be hypothesized that giant hail is occurring in the western white bounded region noted in Figure 3.

d. *2229 UTC*

At this time, a debris ball, or tornadic debris signature (TDS), can be noted as shown in Figure 4. This is about the time the EF-4 tornado was developing and starting cause extensive damage. Looking out into the forward flank of the storm, there is still a broad region of lower CC (~ 0.9) noted by the bounded white line (Figure 4). However, the magnitudes of CC are no longer as low as 0.7. Additionally, Z_{DR} has begun to fill back in with higher values (~ 2-3 dB), but some lower (and negative) values still exist along the edge of the storm. Reflectivity values are still in the 45-55 dBZ range with a few 60 dBZ pixels as has been noted for the past few analysis times. It is possible that giant hail is still occurring in this region, but lack of reports makes it difficult to confirm.

e. *2245 UTC*

The Moore, OK storm at this time is beginning to merge (or be cutoff) with the storm to its south. The primary feature to note here is that there is no longer a broad region of reduced CC (< 0.97) as noted in Figure 5. Also, Z_{DR} has filled back in with values no less than 2 dB. However, reflectivity values are still in the 45-55 dBZ range, though no pixels of 60 dBZ exist anymore. It is possible some small hail is occurring in this region but the threat of giant hail appears to have diminished based on the dual-polarization signatures.

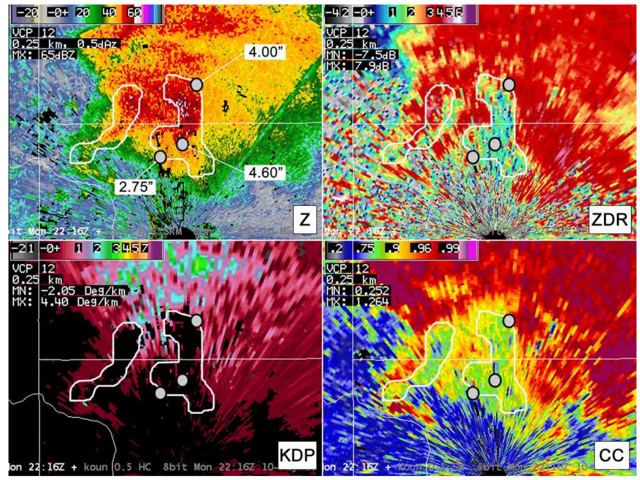

Figure 3: Same as Figure 1, but at 2216 UTC. Gray dots represent storm reports (sizes are noted in Z image; top left). NOTE: There are two bounded white lines for this time period.

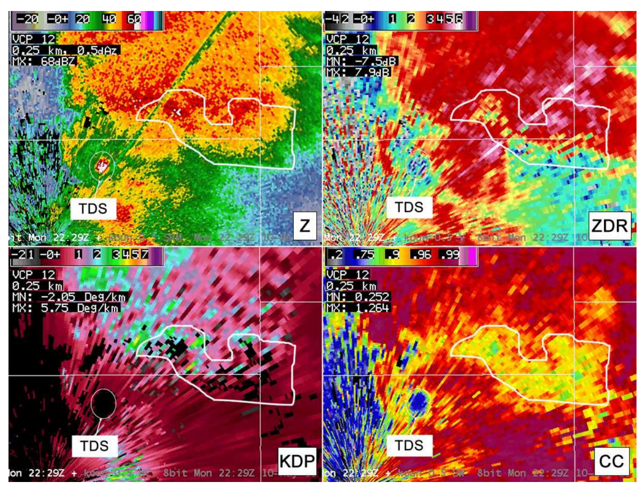

Figure 4: Same as Figure 1, but for 2229 UTC. Note the tornadic debris signature (TDS) at this time frame labeled as so in figure.

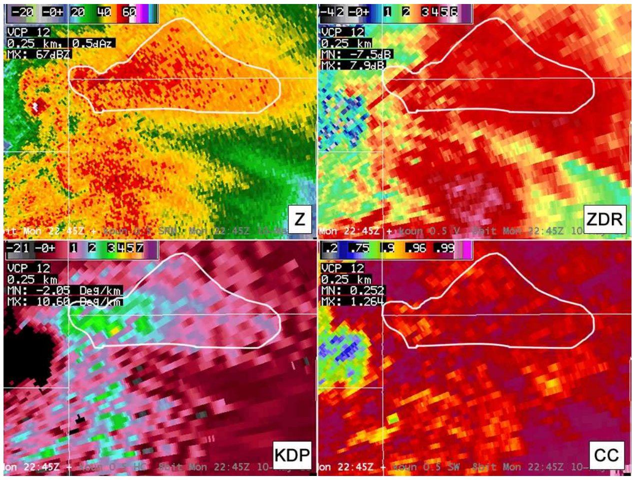

Figure 5: Same as Figure 1, but for 2245 UTC.

4. Discussion & Conclusions

The previous section has presented the evolution of the reflectivity (Z), differential reflectivity (Z_{DR}) and correlation coefficient (CC) fields during the Moore, OK supercell that produced up to softball-sized hail. The primary features to note were that during this evolution reflectivity remained fairly constant (45-55 dBZ) but the dual-polarization variables appeared to evolve with the reports of the largest hail. Prior to the storm having reports of hail, Z_{DR} values were generally greater than 2 dB and CC were greater than 0.97. During the reports of softball-sized hail, Z_{DR} had become noisier and exhibited some negative values while CC became as low as 0.7. At the end of the evolution, the CC became generally greater than 0.97 and Z_{DR} rebounded back to greater than 2 dB.

The transition in Z_{DR} to being noisy with some negative values and the reduction of CC to as low as 0.7 during the time of the largest hail reported agrees well with previous modeling and observational studies by Balakrishnan and Zrnic (1990); Kumjian et al. (2010) and Melnikov et al. (2010). As hail becomes giant ($D > 4$ cm), resonance effects in the horizontal and vertical channels cause Z_{DR} to oscillate. These resonance effects are exacerbated when the hail becomes partially melted and becomes either wet or spongy. It is believed in this case that the hailstones were in a resonance regime due to the noisiness in Z_{DR}. As to the wetness or sponginess, it is believed that the hail was wet due to melting because Balakrishnan and Zrnic (1990) state that CC will not drop significantly for large hail if it is dry, but will drop significantly when large hail becomes wet/spongy. Another explanation for the lower CC could be hail mixed with rain, but personal communication with some eyewitnesses revealed that there was little, if any, rain mixed with the giant hail. As for the relatively constant Z, it is believed that the low concentration of giant hail with lack of rain is leading to the moderately high Z, and not very high Z (~ 70 dBZ).

Future research hopes to employ volumetric analysis to look for signs of giant hail aloft before it reaches the lower-levels. Additionally, this is one case study, and more thorough studies of multiple events is needed to confirm these promising, early results. Overall, it appears promising that noisy, low-to-negative Z_{DR} (< 1 dB) and significantly reduced CC (~ 0.8) in a region of likely hail could alert a forecaster that giant hail is occurring which could be reflected in warning statements to the public.

5. Acknowledgments

The authors would like to thank the Warning Decision Training Branch (WDTB) for providing resources to conduct this research. Also, this extended abstract was prepared by Clark Payne with funding provided by NOAA/Office of Oceanic and Atmospheric Research under NOAA-University of Oklahoma Cooperative Agreement #NA17RJ1227, U.S. Department of Commerce. The statements, findings, conclusions, and recommendations are those of the author(s) and do not necessarily reflect the views of NOAA or the U.S. Department of Commerce.

References

Aydin, K. and Y. Zhao, 1990: A computational study of polarimetric radar observables in hail. *IEEE Trans. Geosci. Remote Sens.*, **28**, 412–421.

Balakrishnan, N. and D. S. Zrnic, 1990: Use of polarization to characterize precipitation and discriminate large hail. *J. Atmos. Sci.*, **47**, 1525–1540.

Bringi, V. N. and V. Chandrasekar, 2001: *Polarimetric Doppler Weather Radar: Principles and Applications*. Cambridge University Press, 636 pp.

Doviak, R. J. and D. S. Zrnic, 1993: *Doppler Radar and Weather Observations*. Academic Press, 562 pp.

Herzegh, P. H. and A. R. Jameson, 1992: Observing precipitation through dual-polarization radar measurements. *Bull. Amer. Meteor. Soc.*, **73**, 1365–1374.

Knight, C. A. and N. C. Knight, 1970: The falling behavior of hailstones. *J. Atmos. Sci.*, **27**, 672–681.

Knight, N. C., 1986: Hailstone shape factor and its relation to radar interpretation of hail. *J. Climate Appl. Meteor.*, **121**, 2223–2238.

Kumjian, M. R., J. C. Picca, S. M. Ganson, A. V. Ryzhkov, J. Krause, D. Zrnic, and A. Khain, 2010: Polarimetric radar characteristics of large hail. *Extended Abstracts, 25th Conf. on Severe Local Storms*, Denver, CO, Amer. Meteor. Soc., 1–14.

Kumjian, M. R. and A. V. Ryzhkov, 2008: Polarimetric signatures in supercell thunderstorms. *J. Appl. Meteor. Climatol.*, **47**, 1940–1961.

Lemon, L. R. and C. A. Doswell, 1979: Severe thunderstorm evolution and mesocyclone structure as related to tornadogenesis. *Mon. Wea. Rev.*, **107**, 1184–1197.

Lemon, L. R., C. D. Payne, C. A. Van Den Broeke, and P. T. Schlatter, 2010: Oklahoma tornadoes of 10 May 2010. *Extended Abstracts, 25th Conf. on Severe Local Storms*, Denver, CO, Amer. Meteor. Soc., 1–10.

Lesins, G. B. and R. List, 1986: Sponginess and drop shedding of gyrating hailstones in a pressure-controlled icing wind tunnel. *J. Atmos. Sci.*, **43**, 2813–2825.

List, R., 1986: Properties and growth of hailstones. *Thunderstorm Dynamics and Morphology*, E. Kessler, Ed., University of Oklahoma Press, 259–276.

Longtin, D. R. et al., 1987: Radar backscattering by large, spongy ice oblate spheroids. *J. Atmos. Oceanic Technol.*, **4**, 355–358.

Mason, B. J., 1971: *The Physics of Clouds*. 2d ed., Oxford University Press, 671 pp.

Melnikov, V. M., R. R. Lee, and N. J. Langlieb, 2010: Hail reflectivity signatures from two adjacent WSR-88Ds: Carrier frequency and calibration issues. *Extended Abstracts, 26th Conf. on IIPS for Metr., Oceanography, and Hydrology*, Atlanta, GA, Amer. Meteor. Soc., 1–9.

Rasmussen, R. M., V. Levizzani, and H. R. Pruppacher, 1984: A wind tunnel and theoretical study of the melting behavior of atmospheric ice particles. Part II: Theoretical study for frozen drops of radius $<500\mu$m. *J. Atmos. Sci.*, **41**, 374–380.

Sachidananda, M. and D. S. Zrnic, 1986: Differential propagation phase shift and rainfall rate estimation. *J. Atmos. Oceanic Technol.*, **21**, 235–247.

Scharfenberg, K. A., et al., 2005: The joint polarization experiment: Polarimetric radar in forecasting and warning decision making. *Wea. Forecasting*, **20**, 775–788.

Steinhorn, I. and D. S. Zrnic, 1988: Potential uses of radar differential phase constant to estimate raindrop and hailstone size distributions. *IEEE Trans. Geosci. Remote Sens.*, **26**, 639–648.

Straka, J. M., D. S. Zrnic, and A. V. Ryzhkov, 2000: Bulk hydrometeor classification and quantification using polarimetric radar data: Synthesis and relations. *J. Appl. Meteor.*, **39**, 1341–1372.

Van Den Broeke, C. A., C. D. Payne, L. R. Lemon, and P. T. Schlatter, 2010: Zdr column characteristics and trends during the 10 May 2010 severe weather outbreak. *Extended Abstracts, 25th Conf. on Severe Local Storms*, Denver, CO, Amer. Meteor. Soc., 1–4.

Zrnic, D. S., V. N. Bringi, N. Balakrishnan, K. Aydin, V. Chandrasekar, and J. Hubbert, 1993: Polarimetric measurements in a severe hailstorm. *Mon. Wea. Rev.*, **121**, 2223–2238.